



SACRED HEART RESEARCH PUBLICATIONS

# Journal of Functional Materials and Biomolecules

Journal homepage: [www.shcpub.edu.in](http://www.shcpub.edu.in)



ISSN: 2456-9429

## SYNTHESIS OF $Mn_3O_4$ AND SHOCK LOADED NANOPARTICLES BY HYDROTHERMAL METHOD

R. Archana<sup>1</sup>, D. Rajkumar<sup>1\*</sup>

Received on 26 November 2023, accepted on 2 December 2023,  
Published online on December 2023

### Abstract

In this work, we report a simple, controlled strategy to prepare manganese oxide nanoparticles ( $Mn_3O_4$  NPs) by hydrothermal method. The prepared sample was subjected to 300 shock pulses. The control and shock loaded  $Mn_3O_4$  NPs were characterized by using different techniques such as x-ray diffraction (XRD), Fourier-transform infrared (FTIR) spectroscopy, UV-Visible spectroscopy and Scanning Electron Microscope (SEM). Powder X-ray diffraction results confirm the crystalline structure of  $Mn_3O_4$  with a tetragonal phase. The surface morphology of control  $Mn_3O_4$  NPs was in unique spherical shape but in the case of shock loaded sample, there is a change of morphology from spherical to rod like morphology, which was confirmed by SEM analysis. FTIR spectra reveals that for 300 shock loaded sample the O-H stretching vanishes. In UV-Vis spectral analysis the band gap for pure  $Mn_3O_4$  is found to be 2.5 eV, for 300 shock loaded sample the band gap is increased and it is found to be 3.2e V.

**Keywords:**  $Mn_3O_4$  NPs, Shock pulses, calcinated.

### 1. Introduction

Nanoscience is the study of condensed materials, properties and behaviors at the nanoscale, optical, chemical, electrical, etc. that are very different from those of bulk materials as well as the fascinating world of bio systems and other natural nanoscale phenomena [1]. In nanoparticles research, the present research activities is mainly focused on metal elements. In that  $Mn_3O_4$  is one of the most useful inorganic oxide materials and it has wide range of applications as well as physical and chemical properties [2-6]. Mn based catalysts particularly  $Mn_3O_4$  is used as a catalyst for the oxidation of methane, carbon monoxide and decomposition of Manganese and it has several oxidation states such as (+2, +3, +4) also have many phases as namely  $MnO$ ,  $MnO_2$ ,  $Mn_2O_3$ ,  $Mn_3O_4$  and  $Mn_5O_8$ . Manganese oxides are attractive non-toxic and inexpensive [7].  $Mn_3O_4$  is the stable one with variety of applications such as MRI (Magnetic resonance imaging), Lithium-ion battery and super capacitors applications due to its theoretical specific capacitance [8-10]. Manganese oxides have been synthesized by using the following methods like sol-gel method, Hydrothermal method, co-

precipitation method and micro-emulsion method etc. Various methods have been there for the synthesis of  $Mn_3O_4$  among them hydrothermal technique is very useful to control the particle size, shape, surface area and structure and this technique does not involve any hazardous element but it produces various morphologies and sizes [11-13].

Shock wave is generated by the abrupt release of energy like in explosion or volcanic eruptions, earthquake and bodies moving at supersonic speeds. It moves faster than the speed of the sound in medium. In recent years, the impact of shock waves on both micro and nano materials shown considerable changes in phase transformation, optical, electrical and magnetic properties. Utilizing all these changes caused by the shock waves, it very possible to tune the structural properties of the materials [14-19].

This work represents the preparation of  $Mn_3O_4$  nanoparticles by Hydrothermal method. Then the prepared sample was subjected to shock pulses. Further the prepared sample was characterized by XRD technique to confirm the material. The functional groups of the prepared sample were observed by FTIR. The energy gap was find out by using UV-Vis spectroscopy and the surface morphology was carried out by using SEM analysis [20].

### Materials and Methods:

All chemicals, such as Manganese sulphate Monohydrate ( $MnSO_4 \cdot H_2O$ ), Potassium Permanganate ( $KMnO_4$ ), Ethanol and Double distilled water were procured from Sigma Aldrich.

### Synthesis of $Mn_3O_4$ Nanoparticles:

For the synthesis of  $Mn_3O_4$  nanoparticles, 0.15 M of potassium permanganate and 0.07 M of manganese sulphate were prepared separately in double distilled water under magnetic stirring. Manganese sulphate solution was slowly added into potassium permanganate solution and stirred for half an hour. The mixture was transferred into a Teflon-Lined stainless steel autoclave with 80 ml capacity. The autoclave was sealed and kept in

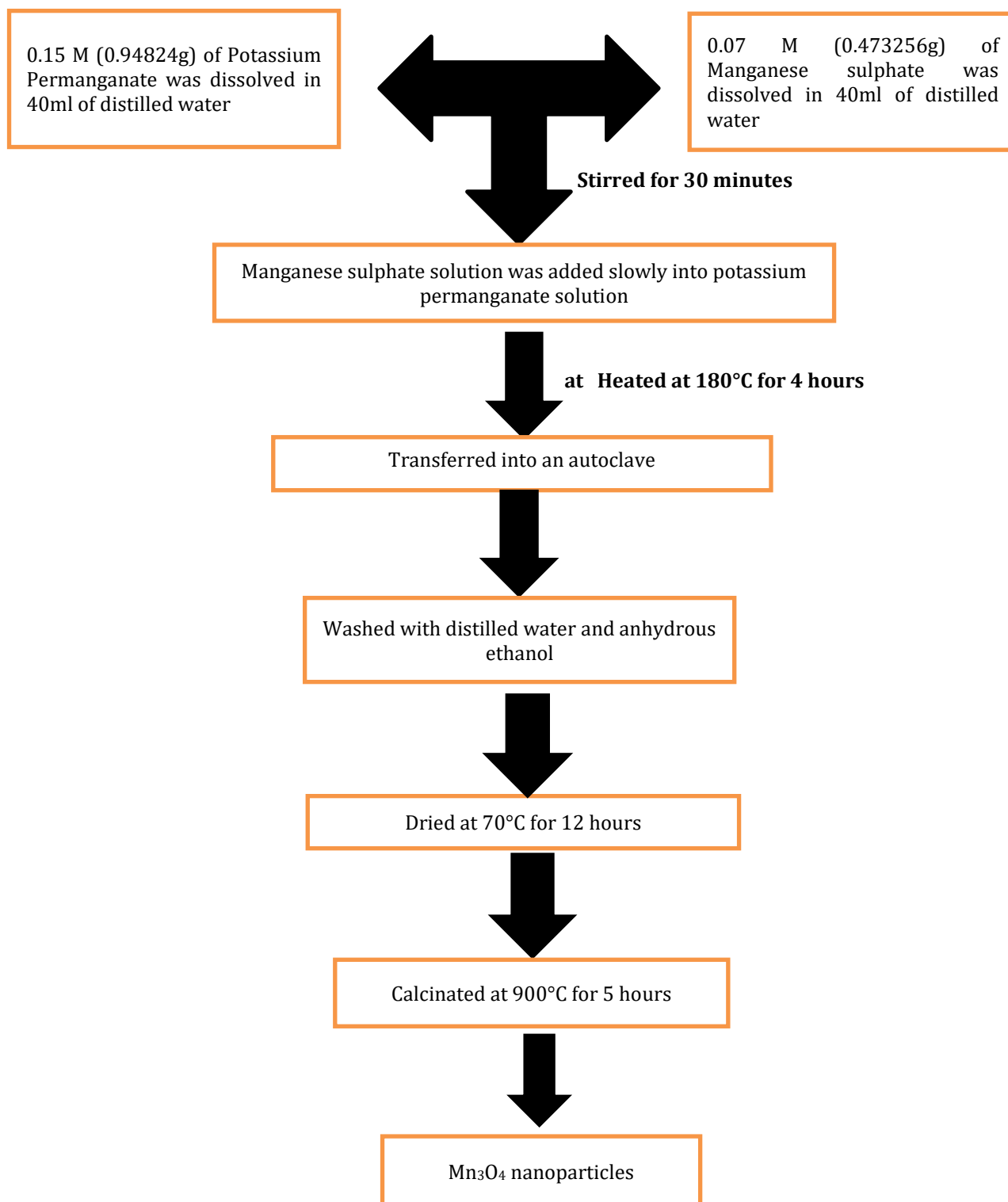
\*Corresponding Author e-mail: [rajikumar@shcpt.edu](mailto:rajikumar@shcpt.edu)

\*Sacred Heart College (Autonomous), Tirupattur – 635601, Tamil Nadu, India.

an electric oven for 24hrs at 160°C. The precipitate was then collected after being cooled to room temperature. The precipitate was washed with deionized water and anhydrous ethanol for multiple times. Then, the hydrothermally synthesized precipitate was dried at 70°C for 12 hr. Finally, the dried precipitate was ground with mortar and pestle and it was calcinated at 900°C for 5hr in

the muffle furnace. Finally, the dark brown powder was obtained and named as Mn<sub>3</sub>O<sub>4</sub> nanoparticles.

The un calcinated sample was then subjected to 300 shocks. The comparative study was carried out between control and shock wave loaded Mn<sub>3</sub>O<sub>4</sub> nanoparticles. The pictorial representation for the synthesis of Mn<sub>3</sub>O<sub>4</sub> nanoparticles is shown below.



## Results and Discussion

### Powder X-ray diffraction:

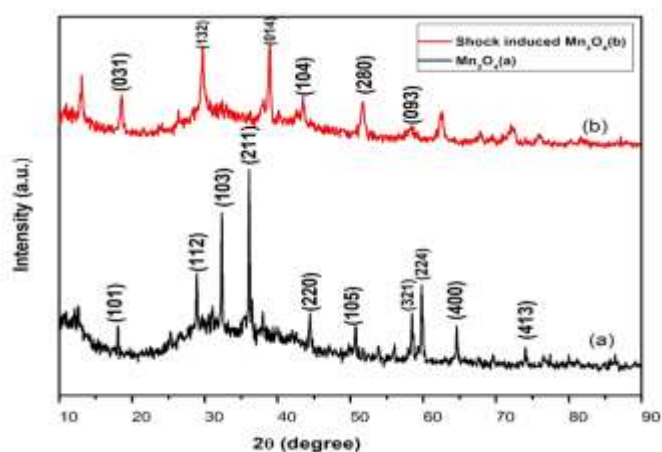
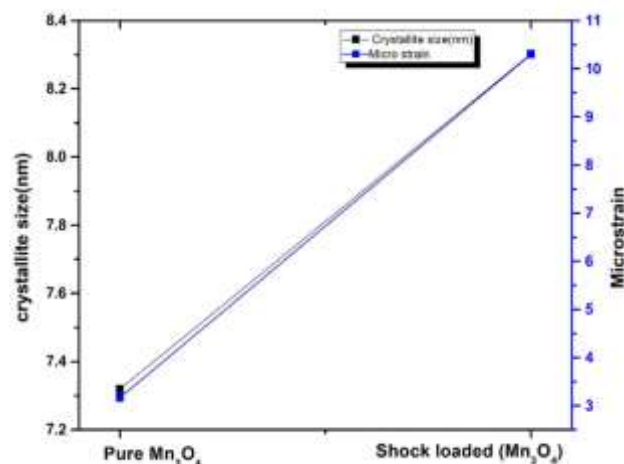


**Fig: 3. 1 Powder XRD pattern of pure and shock Induced Mn<sub>3</sub>O<sub>4</sub> nanoparticle**

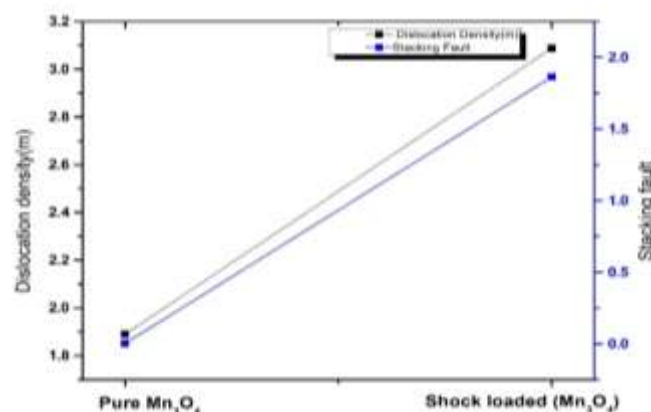
Figure: 3.1 shows that the X-Ray Diffraction pattern of pure and shock induced Mn<sub>3</sub>O<sub>4</sub> nanoparticles. The diffraction peaks are matched with JCPDS card No:24-0734. The obtained peak positions for pure Mn<sub>3</sub>O<sub>4</sub> is  $2\theta = 18.08^\circ, 28.89^\circ, 32.32^\circ, 36.08^\circ, 44.43^\circ, 50.72^\circ, 58.45^\circ, 59.79^\circ, 64.57^\circ, 74.04^\circ$  similarly for shock loaded sample is  $2\theta = 18.60^\circ, 29.69^\circ, 39.05^\circ, 43.34^\circ, 51.66^\circ$  and corresponding crystal planes for pure Mn<sub>3</sub>O<sub>4</sub> (101), (112), (103), (211), (220), (105), (321), (224), (400), (413) and for shock induced Mn<sub>3</sub>O<sub>4</sub> (031), (132), (014), (104), (280), (093). The results shows that the synthesized Mn<sub>3</sub>O<sub>4</sub> NPs are in tetragonal structure [21]. The high phase purity of the prepared Mn<sub>3</sub>O<sub>4</sub> sample is because there is no evidence for the presence of any other oxidation states of Manganese and the prepared Mn<sub>3</sub>O<sub>4</sub> particle size should be small, because the resulting diffraction peaks are quite broad and of low intensity [22]. The as-synthesized sample was then subjected to 300 shock pulses. The XRD pattern of shock loaded sample reveals that there is a phase transition from Mn<sub>3</sub>O<sub>4</sub> to Mn<sub>2</sub>O<sub>7</sub> (i.e.,) tetragonal to monoclinic due to impact of 300 shocks with Mach number 2.2. The XRD patterns of shock loaded sample well matches with the JCPDS card no: 79-0083. The average crystallite size of Mn<sub>3</sub>O<sub>4</sub> NPs and shock loaded sample was found to be 7.3 nm and 4.9 nm respectively.

| Sample                                       | Average Crystallite Size |
|--|--------------------------|
|  | (D)<br>(nm)              |
| Pure Mn <sub>3</sub> O <sub>4</sub>          | 7.3                      |
| Shock Induced Mn <sub>3</sub> O <sub>4</sub> | 4.9                      |



**The above figure shows graph versus crystalline size and Micro strain.**

From the plot, it is clear that the crystalline size decreases, micro strain decreases.



**The above figure shows the plot versus Dislocation density and stacking fault**

From the plot, it is clear that as the Dislocation density increases, stacking fault also increases.

### FTIR Analysis:

Figure: 3.2 shows that the FTIR spectra for pure Mn<sub>3</sub>O<sub>4</sub> and Shock loaded Mn<sub>3</sub>O<sub>4</sub> nanoparticles. For pure Mn<sub>3</sub>O<sub>4</sub>, the absorption band at 3315 cm<sup>-1</sup> is attributed to O-H stretching mode and the absorption peak exists near around 1634, 1511, and 1321 cm<sup>-1</sup> could be attributed to O-H bending vibration combined with Mn atoms. The peak located at 597 and 511cm<sup>-1</sup> were associated with the coupling mode between the Mn-O vibration mode of tetrahedral site and peaks at 472, 406 cm<sup>-1</sup> correspond to octahedral sites. For 300 Shock loaded sample, the intensity of these peaks have almost vanished and this effect shows that the properties of Mn<sub>3</sub>O<sub>4</sub> nanoparticles changes gradually. The characteristic narrow band situated at 1622 cm<sup>-1</sup> correspond to the hydroxy (OH), should be absorbed by the samples or KBr. The peak at 1271 cm<sup>-1</sup> indicates N-O stretching mode, peak at 695cm<sup>-1</sup> corresponds to Mn-O stretching mode, peaks at 549 and 503 cm<sup>-1</sup> associated to the Mn-O distortion vibration [23].

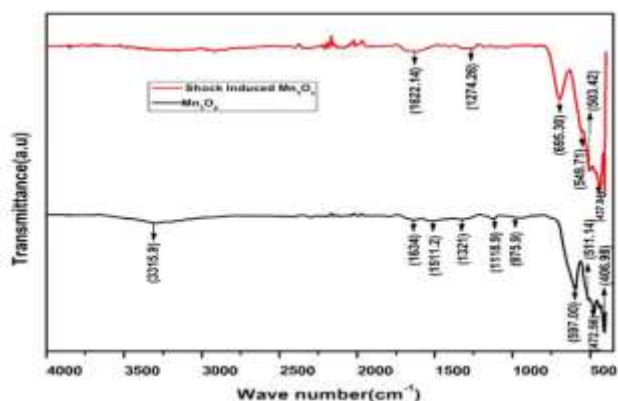


Fig. 3.2 FTIR Spectra of  $Mn_3O_4$  and Shock Induced  $Mn_3O_4$

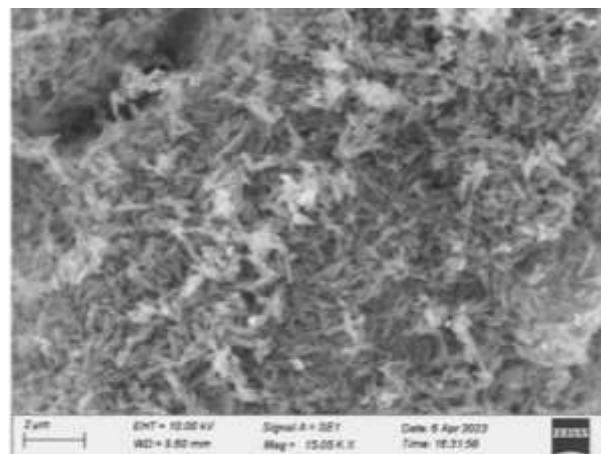


Fig 3.4: SEM images of (a) control  $Mn_3O_4$  (b) shock wave loaded  $Mn_3O_4$

### UV-Vis Analysis:

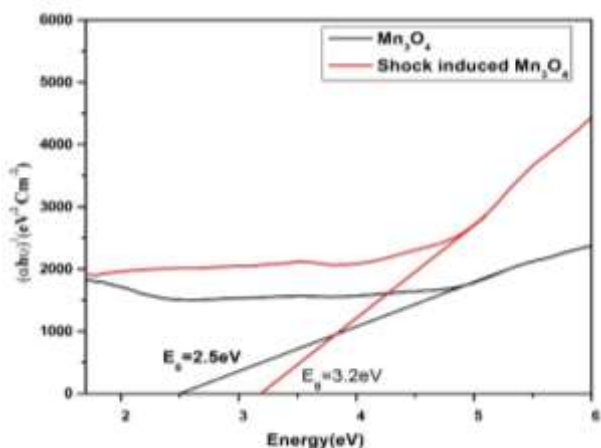
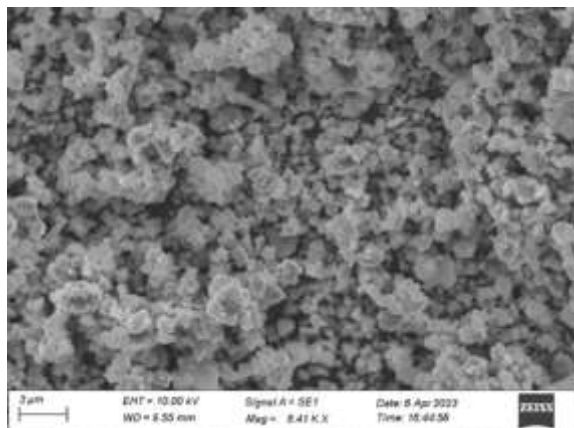


Fig 3.3 shows that the UV-Vis Spectrum for pure and shock loaded  $Mn_3O_4$

For control  $Mn_3O_4$ , the value of band gap is found to be 2.5 eV and for shock loaded  $Mn_3O_4$ , the band gap is found to be 3.2 eV. The change in band gap is due to the reduction of  $KMnO_4$  by ethanol to manganese and the oxidation state decreases from  $Mn^{7+}$  to  $Mn^{3+}$ . As  $Mn^{3+}$  is a much stable state of manganese, very small amount of Mn gets further reduced to  $Mn^{2+}$  states and these changes may be due to the changes in the structural properties of the sample.

### SEM ANALYSIS:



The surface morphology of control and shock wave loaded  $Mn_3O_4$  nanoparticles were analyzed using SEM analysis. Fig. (a), show the aggregated  $Mn_3O_4$  nanoparticles are in the form of spherical morphology. The size of the control  $Mn_3O_4$  nanoparticles are in the range of 40-50nm and it is in good agreement with the XRD results. But in the case of shock loaded sample, there is a change of morphology from spherical to rod like morphology with less agglomeration. The change in morphology may be due to the propagation of shock wave in the sample.

### Conclusion:

We conclude that the pure  $Mn_3O_4$  NPs and shock Induced  $Mn_3O_4$  NPs was successfully prepared by hydrothermal method. The Pure and shock induced  $Mn_3O_4$  NPs were characterized by XRD, FTIR, UV-Vis and SEM Analysis. The XRD pattern reveals that there is a phase transition from tetragonal to monoclinic structure is due to the impact of shock pulses and there is a change in crystallite size. FTIR spectra reveals that for 300 shock loaded sample the O-H stretching vanishes. In UV-Vis spectral analysis the band gap for pure  $Mn_3O_4$  is found to be 2.5 eV ,for 300 shock loaded sample the band gap is increased and it is found to be 3.2e V. The SEM analysis shows that in case of shock loaded sample, there is a change in morphology from spherical to rod structure.

### References:

- [1] G. Ali Mansoori An Introduction to Nanoscience and Nanotechnology DOI 10.1007/978-3-319-46835-8\_1
- [2] Moggridge GD, Rayment T, Lambert RM. J Catal 1992:134:161.
- [3] Stobhe ER, Boer BAD, Deus JW.Catal 1996:47:161.
- [4] Yamashita T, Vannice A. J Catal Today 1999:163:158.
- [5] Wang WM, Yang YN, Zhang JY, Appl Catal A 1995:133:81.
- [6] Baldi M, Finocchio E, Millella F, Busca G. Appl Catal B 1998;16:43.
- [7] Euna, J., Changsoo, K. and Soonchil, L. (2011)  $^{55}Mn$  Nuclear Magnetic Resonance for Antiferromagnetic  $\alpha$ - $Mn_3O_4$ . *New Journal of Physics*, 13, Article ID:013918.

- [8] M.R. Kumar et al., Large scale production of SrFe<sub>12</sub>O<sub>19</sub> nanoparticles with low calcination temperature. *Mater. Res. Express* 4, 095007 (2017).
- [9] M.R. Kumar, R.Y. Hong, Effect of surfactants on SrM Core-Shell nanoparticles synthesised at low temperature. *Micro Nano Lett.* 12, 289 (2017).
- [10] K.S. Kang et al., Electrodes with high power and high capacity for rechargeable lithium Batteries. *Science* 311, 977 (2006).
- [11] Raj ,B.G.S., Asiri, A.M., Wu, J.J. and Anandan, S., "Synthesis of Mn<sub>3</sub>O<sub>4</sub> nanoparticles via chemical precipitation approach for supercapacitor application," *Journal of Alloys and Compounds*, 636, 234-240. 2015.
- [12] M. Tsuji, S. Gomi, Y. Maeda, M. Matsunaga, S. Hikino, K.Uto, T. Tsuji, H. Kawazumi, Rapid Transformation from Spherical Nanoparticles , Nanorods, Cubes, or Bipyramids to Triangular Prisms of silver with PVP, Citrate and H<sub>2</sub>O<sub>2</sub>, *Langmuir* 28 (2012) 8845-8861.
- [13] T. Parnklang, C Lertvachirapaiboon, P. Pienpinijtham, K. Wongravee, C.Thammacharoen, S. Ekgasit, H<sub>2</sub>O<sub>2</sub>-triggered Shape transformation of silver Nanospheres to Nanoprisms with controllable longitudinal LSPR Wavelength, *RSC Adv.* 3 (2013) 12886-12894.
- [14] Zhi Su, William L. Shaw, Yu-Run Miao, Sizhu You, Dana D. Dlott, and Kenneth S. Sulicks Shock wave chemistry in a metal -organic framework. *J. Am. Chem. Soc.* 139, 4619-4622 (2017).
- [15] A. Sivakumar , C. Victor, M. Muralidhr Nayak, S.A. Martin Britto Dhas. Structural, Optical, and morphological stability of ZnO nanorods under shock wave loading conditions *Mater. Res. Express* 6, 045031 (2019).
- [16] Yan Qiu Zhu, Toshimori Sekine, Yan Hui Li, Michael W. Fay, Yi Min Zhao, C.H. Patrik Poa, Wen Xin Wang, Martin J. Roe, Paul D. Brown, Niles Fleischer and Reshef Tenne. Shock-absorbing and failure mechanisms of WS<sub>2</sub> and MoS<sub>2</sub> nanoparticles with fullerene-like structures under shock wave pressure *J. Am. Chem. Soc.* 127. 16263-16272 (2005).
- [17] Vishakantiah Jayaram, Asha Gupta, K.P.J. Reddy. Investigation of strong shock wave interactions with CeO<sub>2</sub> ceramic *Journ. Adv. Ceramic* 3, 297-305 (2014).
- [18] S. Kalaiarasi, A. Sivakumar, S.A. Martin Britto Dhas, M. Jose. Shock wave induced anatase to rutile TiO<sub>2</sub> phase transition using pressure driven shock tube. *Mater. Lett* 219, 72-75 (2018).
- [19] V. Jayaram and K.P.J. Reddy. Experimental study of the effect of strong heated test gases with cubic zirconia. *ADV. Mater. Lett.* 7, 100-150 (2016).
- [20] Sharrouf, M., Awad, R., Roumie, M. and Marhaba, S. (2015) Structural, Optical and Room Temperature Magnetic study of Mn<sub>2</sub>O<sub>3</sub> Nanoparticles. *Materials Sciences and Applications*, 6, 850-859.
- [21] G. An, P. Yu, M. Xiao, Z. Liu, Z. Miao, K. Ding and L. Mao, *Nanotechnology* 19 (2008) 1-7.
- [22] Y. Li, H. Tan, X.Y. Yan, B. Goris, J. Verbeeck, S. Bals, P. Colson, R. Cloots, G.V. Tendeloo and B.L. Su, *Small* 7 (2011) 475-483.
- [23] Versiani, A.F., Andrade, L.M., Martins, E.M., Scalzo, S., Geraldo, J.M., Chaves, C.R., Ferreira, D.C., Ladeira, M., Guatimosim, S., Ladeira, L.O. and da Fonseca, F.G., "Gold nanoparticles and their applications in biomedicine," *Future Virology*, 11(4). 293-309. 2016.
- [24] Ahmed A. Amer, S.M. Reda, M.A. Mousa and Mohamed Mokhtar Mohamed *RSC Adv.*, 2017, 7, 826. DOI: 10.1039/c6ra24815b.
- [25] Yumin Wang<sup>1</sup> . Chao Hou<sup>1</sup> . Xiaohui Lin<sup>1</sup> . Hongli Jiang<sup>1</sup> . Cuijin Zhang<sup>2</sup> . Guizhen Liu<sup>3</sup>. *Applied Physics A* (2021) 127:277.